

論文の内容の要旨

Direct mass measurements of neutron-rich Ca isotopes (中性子過剰 Ca 同位体の直接質量測定)

氏名 小林 幹

We have performed the first direct mass measurements of neutron-rich calcium isotopes beyond neutron number $N = 34$ at the RIKEN Radioactive Isotope Beam Factory (RIBF) using the time-of-flight magnetic-rigidity (TOF- $B\rho$) technique. The masses of very neutron-rich nuclei in the vicinity of ^{54}Ca have been measured with precisions almost as high as the best previously reached by TOF- $B\rho$ mass spectrometry.

The mass of atomic nuclei is a fundamental quantity as it reflects the sum of all interactions within the nucleus. Changes in the shell structure in nuclei far from stability, called “shell evolution”, can be probed by mass measurements. Particularly, the presence of subshell gaps at $N = 32$ and 34 in the isotopes around calcium has attracted much attention over recent years. Mass measurements of neutron-rich nuclei in the vicinity of $N = 32$ and 34 , including $^{55-57}\text{Ca}$, ^{54}K , and $^{50-52}\text{Ar}$, provide pivotal information for discussing the shell evolution at $N = 32$ and 34 .

To investigate the shell evolution at $N = 32$ and 34 , the experiment was performed at RIBF by using the High-Resolution Beam Line and the SHARAQ spectrometer. Masses were deduced by the TOF- $B\rho$ technique. For the most exotic nuclides, the TOF mass measurement is the only direct method to progress towards the drip line and investigate the more exotic shell effects. The TOF of an ion was measured by a pair of the diamond detectors with extremely high time resolutions, which were newly developed for the mass

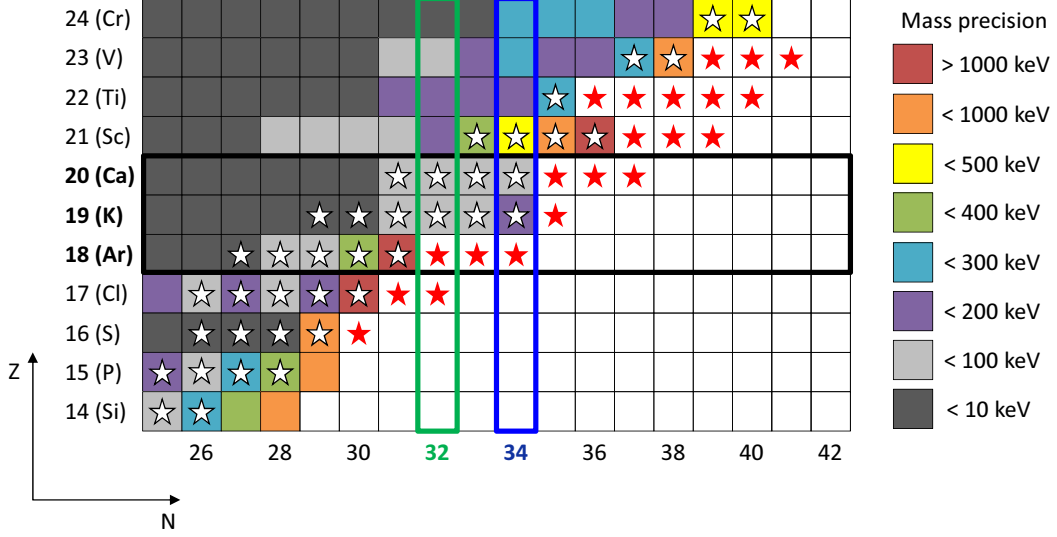


Figure 1: Nuclear chart in the vicinity of neutron-rich Ca isotopes. Filled colors show the mass uncertainties in the literature. Stars represent the nuclei whose masses are measured in the present experiment. Filled red stars indicate the nuclei with unknown masses.

measurements. The dispersion-matched operation of the High-Resolution Beam Line and the SHARAQ spectrometer allowed high-precision measurement of the beam momentum.

Figure 1 shows the nuclear chart near the neutron-rich Ca isotopes. The stars represent the nuclei observed in the present experiment, and the filled red stars indicate the nuclei whose masses were measured for the first time in the present experiment. The masses of 21 nuclei ($^{62-64}\text{V}$, $^{58-62}\text{Ti}$, $^{58-60}\text{Sc}$, $^{55-57}\text{Ca}$, ^{54}K , $^{50-52}\text{Ar}$, $^{48,49}\text{Cl}$, and ^{46}S) were determined for the first time. In addition, the uncertainties of 10 masses (^{61}V , $^{55-57}\text{Sc}$, $^{48,49}\text{Ar}$, ^{47}Cl , ^{45}S , and $^{42,43}\text{P}$) were reduced by more than 100 keV. Figure 2 shows the systematics of the two-neutron separation energies S_{2n} between the neutron numbers $N = 27$ and $N = 41$ from P ($Z = 15$) to V ($Z = 23$) isotopes including our new results. The typical mass resolution in the present experiment was $\sigma_m/m = 1.0 \times 10^{-4}$, and the mass uncertainty of $\delta m/m = 2.6 \times 10^{-6}$ was achieved. The present mass measurements have demonstrated the excellent performance of our experimental system in terms of achieved mass uncertainties and distance from stability of the measured nuclei, compared with other TOF mass measurement facilities. Direct mass measurements using the TOF- $B\rho$ technique have been carried out for the first time at RIBF, and the present work has established TOF mass measurements as an excellent application of this facility.

The magnitude of the shell gaps at $N = 32$ and 34 has been evaluated from the

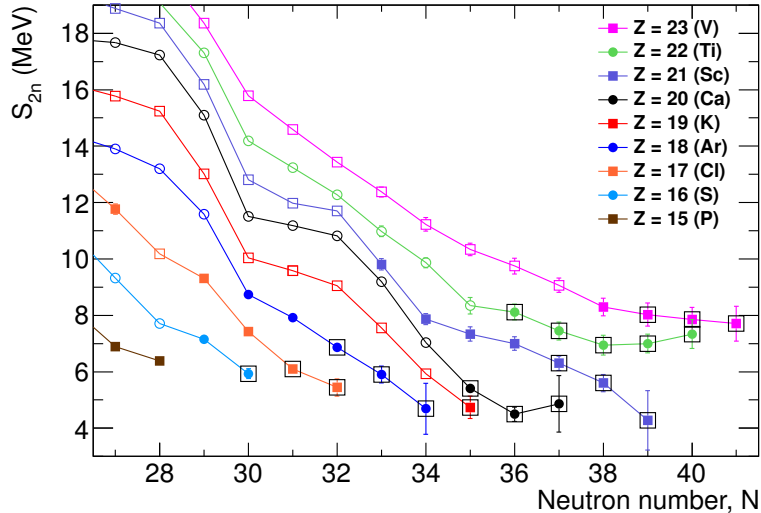


Figure 2: The two-neutron separation energy S_{2n} plotted for neutron numbers $N = 27$ –41 from P ($Z = 15$) to V ($Z = 23$) isotopes. Open symbols show S_{2n} values from the literature. The S_{2n} values calculated with the results in the present work are shown as filled symbols. Squares surrounding the filled symbols show the S_{2n} values measured for the first time in the present experiment.

experimentally determined masses using the difference of the three-point mass differences $[\Delta_3(N)]$ at adjacent even- N and odd- N . Figures 3(a) and (b) show the systematics of the shell gaps ($\delta e^-(N) \equiv 2[\Delta_3(N) - \Delta_3(N-1)]$) for the Ca and Ar isotopes, respectively, and Figs. 4(a) and (b) show that along the $N = 34$ and $N = 32$ isotonic chains, respectively. For the Ca isotopes, the magnitude of the shell gap at $N = 34$ is similar to that at $N = 32$ as shown in Fig. 3(a). Moreover, the increase in the $N = 34$ shell gap at $Z = 20$ (Ca) along the $N = 34$ isotonic chain is comparable to the $N = 32$ shell gap at $Z = 20$ along the $N = 32$ chain, as shown in Fig. 4. These experimental results provide strong evidence for the presence of a sizable $N = 34$ subshell gap in ^{54}Ca similar in magnitude to that for $N = 32$. This is consistent with the result in the previous γ -ray spectroscopy in ^{54}Ca , which first reported experimentally the onset of the $N = 34$ subshell gap. In contrast, for the argon isotopes, there is no significant increase in the subshell gap at $N = 32$ relative to $N = 30$ as shown in Fig. 3(b), and a weakening of the $N = 32$ gap is indicated below the calcium and potassium isotopes as shown in Fig. 4(b).

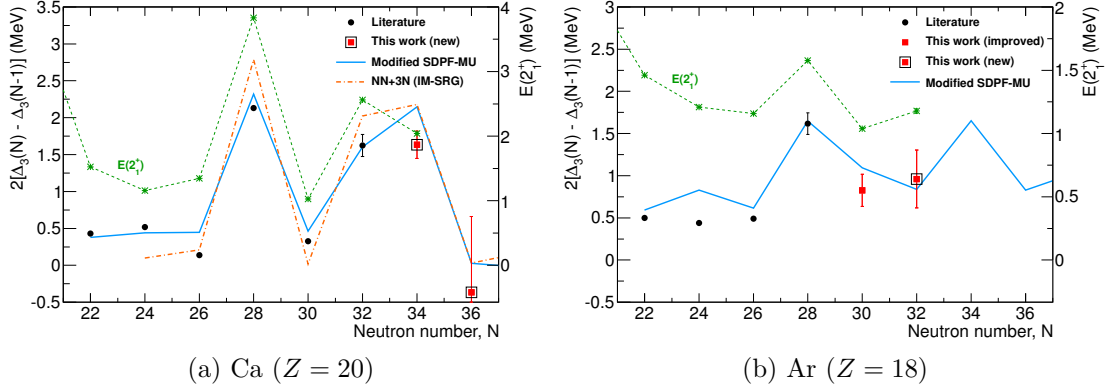


Figure 3: The shell gaps $\delta e^-(N) = 2[\Delta_3(N) - \Delta_3(N-1)]$ for the (a) Ca and (b) Ar isotopes as a function of neutron number. Red squares show the results in which uncertainties are improved by more than 100 keV. Squares surrounding the filled red symbols show the new results.

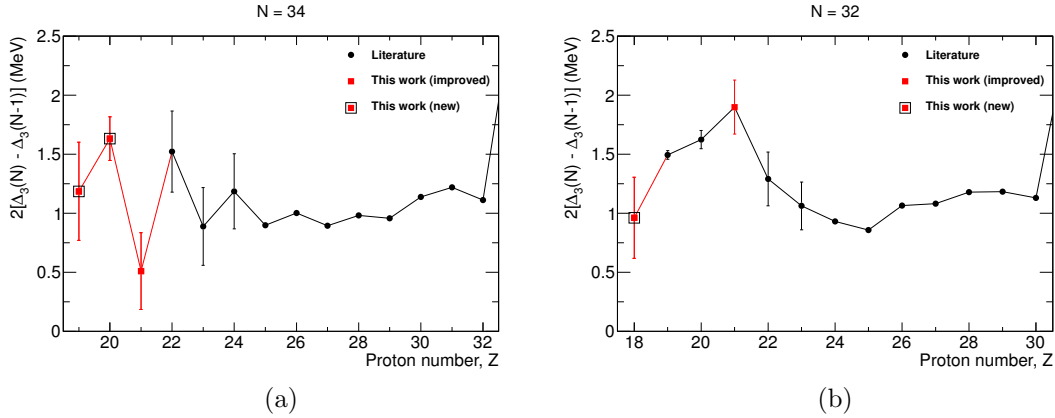


Figure 4: The shell gaps $\delta e^-(N) = 2[\Delta_3(N) - \Delta_3(N-1)]$ at (a) $N = 34$ and (b) $N = 32$ as a function of proton number Z . Red squares at $Z = 21$ in (a) and (b) show the results in which uncertainties are improved by more than 100 keV and 70 keV, respectively. Squares surrounding the filled red symbols show the new results in the present experiment.